Soft Matter

Cite this: *Soft Matter*, 2011, **7**, 7359

www.rsc.org/softmatter

PAPER

Influence of chirality on the modes of self-assembly of 12-hydroxystearic acid in molecular gels of mineral oil†

Douglas A. S. Grahame,[a] Caitlin Olauson,[a] Ricky S. H. Lam,[a] Tor Pedersen,[b] Ferenc Borondics,[b] Shibu Abraham,[c] Richard G. Weiss[c] and Michael A. Rogers*[d]

Received 25th April 2011, Accepted 9th June 2011
DOI: 10.1039/c1sm05757j

The gelating abilities of enantiopure, racemic, and different *enantio*-enriched mixtures of 12-hydroxystearic acid (12HSA) have been compared in order to clarify conflicting reports in the literature (1) concerning their ability to gelate organic liquids. Less than 1.0 wt % of optically pure (D)-12HSA was found to gelate mineral oil. The gel matrix was comprised of high aspect ratio fibers in which the 12HSA molecules were organized as head-to-head dimers and the 12-hydroxyl groups formed an H-bonding network along the axis transverse to the longitudinal growth. Below 2 wt %, racemic 12HSA in mineral oil did not reach the percolation threshold. Its organogels were comprised of platelet-like crystals with a molecular arrangement of single, in-plane, hydrogen-bonded acyclic dimers that prevent longitudinal growth and limit the ability of the polar groups to phase separate during nucleation.

Introduction

The ability of a low molecular weight organogelators (LMOGs) to form rod-like structures is related to a subtle balance among several contrasting parameters which control its solubility in a given liquid and its epitaxial growth patterns.[1,2] Self-assembled fibrillar networks (SAFiNs), unlike platelet-based assemblies such as those found in many fatty acids, fatty alcohols and waxes, are comprised of objects with a single elongated axis. It has been established that LMOG chirality can be an important aspect of how SAFiNs are organized at both the molecular and supramolecular levels.[3] In LMOGs with at least one stereo centre, chirality can be expressed at length scales much larger than the molecular sizes, even in the supramolecular assemblies including rod, tape or tubular morphologies.[3]

12-Hydroxystearic acid (12HSA) has been widely studied as a model system for organogelation due, in part, to its structural simplicity.[1a,4] The sense of supramolecular twist of optically pure 12HSA can be correlated with the chirality of the enantiomer (*i.e.*, D -12HSA forms left-handed helices).[4g] Upon cooling the sol of a SAFiN, gelation is initiated by the nucleation of the gelator and subsequent crystal growth of the fiber.[5] During crystal growth, dissolved gelator molecules, either individually or as aggregates, diffuse and accrete onto a growing crystal surface. Growth may result in one-, two-, or three-dimensional crystals depending on the relative rates at which the dissolved molecules adhere to different surfaces of nucleated species.

This manuscript addresses three primary questions regarding the role of molecular chirality of 12HSA and its molecular gels:

(1) What are the differences between the aggregate structures from racemic and optically pure 12HSA?

(2) How do the differences between the supramolecular assemblies of racemic and *enantio* pure 12HSA influence the properties of their organogels?

(3) When enantiomers of 12HSA are mixed in different proportions, what is the resulting morphology of the supramolecular assemblies and in their gels?

Although some aspects of these questions have been addressed recently by Sakurai *et al.*[1b] who used solid-state NMR to identify two types of hydrogen bonding for D-HSA and DL-HSA. Here, we have examined the nucleation phenomena by time-dependent synchrotron IR measurements and optical microscopy, and have extended the range of *enantio* mixtures to determine at what point the morphology of the SAFiNs changes. The results reported here demonstrate how the nucleation and growth processes differ among the *enantio* pure, *enantio*-enriched, and racemic mixtures of 12HSA and lead to different gelating abilities.

Experimental part

Materials

Heavy mineral oil (Sigma-Aldrich, Oakville, ON, CAN), ethanol (Sigma-Aldrich, anhydrous), ethyl acetate (Sigma-Aldrich,

[a]*Department of Food and Bioproduct Science, University of Saskatchewan, 51 Campus Dr, Saskatoon, SK, S7N5A8, Canada*
[b]*Canadian Light Source, Saskatoon, SK, S7N 0X4, Canada*
[c]*Department of Chemistry, Georgetown University, Washington, DC, 20057-1227, USA*
[d]*Department of Food Science, Rutgers University, The State University of New Jersey, New Brunswick, NJ, 08901, USA. E-mail: rogers@AESOP.Rutgers.edu*

† Electronic supplementary information (ESI) available. See DOI: 10.1039/c1sm05757j

HPLC grade), acetone (Sigma-Aldrich, HPLC grade), $Na_2Cr_2O_7 \cdot 2H_2O$ (J.T. baker, >99%), conc. H_2SO_4 (Mallinckrodt, >95%), DMSO (Fischer, 99.9%), and sodium borohydride (Aldrich, 99%) were used as received. (*R*)-12-Hydroxystearic acid, the D-enantiomer[1b] (D-12HSA), was used as received from Sigma-Aldrich (Oakville, ON, CAN) or purified from material received from Arizona Chemical Company by 3 recrystallizations from 1 : 19 ethyl acetate:hexane to yield a white solid, mp 78.5–80.8 °C (lit. 80.2–82.1 °C).[4d]

Synthesis of racemic (DL)-12-hydroxystearic acid

D-12HSA (3.0 g, 10 mmol) was added to a stirred solution of $Na_2Cr_2O_7$ (2.1 g, 7.0 mmol) in DMSO. Conc. H_2SO_4 (2.0 g, 2.5 eq) was added dropwise with stirring, maintaining the temperature below 80 °C. The mixture was heated and stirred at 70 °C for 2 h and stirred for an additional 12 h at ambient temperature. The reaction mixture was poured into ice-cold water and the solid that precipitated was filtered. The solid was chromatographed using a silica gel column and 1 : 9 ethyl acetate:hexane as eluent. After recrystallization from acetone, 1.0 g (33%) of 12-oxooctadecanoic acid was obtained as an off-white solid, mp 78.7–81.4 °C. ^{1}H NMR ($CDCl_3$, 400 MHz), δ 0.86–0.90 (m, 3H), 1.27–1.65 (m, 24H), 2.33–2.40 (m, 6H); ~99% by GC.

The 12-oxooctadecanoic acid was reduced to DL-12HSA by $NaBH_4$ in ethanol.[6] In a typical reaction, 12-oxooctadecanoic acid (1 g, 3 mmol) was added to 25 mL absolute ethanol with stirring at room temperature. The solvent was warmed slightly to dissolve the compound. Sodium borohydride (0.1 g, 3 mmol) was then added and the mixture was stirred at room temperature for 1.5 h. Excess sodium borohydride was destroyed by neutralizing with glacial acetic acid. The ethanol and acetic acid were removed under vacuum and the yellowish-white residue was dried under vacuum for an additional 12 h. It was washed with water (4 × 30 mL), dried, and recrystallized from acetone to yield 0.90 g (96%) of DL-12HSA, mp 74.9–76.9 °C (lit. mp 76.2 °C).[1b] ^{1}H NMR ($CDCl_3$, 400 MHz), δ 0.87–0.90 (t, 3H, J = 6.6 Hz), 1.28–1.65 (m, 28H), 2.17–2.36 (t, 2H, J = 7.4 Hz), 3.58–3.60 (m, 1H); IR (neat) 3327, 2915, 2849, 1706, 1464, 1436, 1410, 1328, 1314, 1295, 1277, 1263, 1241, 1222, 1189, 1133, 1116, 1081, 1026, 1000, 920, 898, 861, 837, 794, 728, 721, 684, 631, 619, 605 cm^{-1}. Analytical data for $C_{18}H_{36}O_3$; C 71.95, H 12.08, (Calculated); C 71.54, H 12.62 (Observed).

Instrumentation

^{1}H NMR spectra were recorded on a Varian 400 MHz spectrometer with tetramethylsilane as the internal standard. Gas chromatograms were obtained on 5890 HP chromatographs with an Alltech DB-5 (0.25 μm, 30 m × 0.25 mm) column and flame ionization detectors. IR spectra were recorded on a Perkin-Elmer Spectrum One FTIR spectrometer interfaced to a computer, using attenuated total reflection accessory plates. Elemental analyses were carried out on a Perkin-Elmer PE2400 microanalyzer. Polarized light micrographs were acquired using a Nikon Eclipse E400 light microscope equipped with a Nikon DS-FiL color camera and a long working distance 10X lens and condenser with a resolution of 2560 by 1920. A drop of solution/sol was placed on a glass slide and quench cooled to 30 °C using a temperature-controlled stage (LTS 120 and PE94 temperature controller (Linkam, Surrey, United Kingdom).

Fourier transform infrared (FTIR) spectra were collected using the end station of the mid-IR synchrotron beamline (beamline 01B1-01, Canadian Light Source, Saskatoon, SK). The end station is comprised of a Bruker Optics IFS66v/S interferometer coupled to a Hyperion 2000 IR microscope (Bruker Optics, Billerica, MA, USA). Light is focused on the sample using a 15X magnification Schwarzschild condenser, collected by a 15X magnification Schwarzschild objective with the aperture set to a spot size of 40 μm × 40 μm and detected by a liquid nitrogen cooled narrowband MCT detector utilizing a 100 μm sensing element.

A KBr-supported Ge multilayer beam splitter was used to measure spectra in the mid-infrared spectral region. Measurements were performed using OPUS 6.5 software (Bruker Optics, Billerica, MA). The measured interferograms were an average of 32 scans and were recorded by scanning the moving mirror at 40 kHz (in relation to the reference HeNe laser wavelength of 632.8 nm). The wavelength range collected was 690–7899 cm^{-1} with a spectral resolution of 4 cm^{-1}. Single channel traces were obtained using the fast Fourier transform algorithm, without any zero-filling, after applying a Blackman–Harris 3-Term apodization function. For single spectra, measurements of reference single channel traces were carried out in the sol state.

Methods

Samples were prepared at 0.5, 1.0, 1.5, and 2.0 wt % to determine the critical gelation concentrations. Samples containing 2.5 wt % of different mixtures of D-12HSA and DL-12HSA in mineral oil were prepared in triplicate by heating to 100 °C for 30 min and then quench-cooling (*i.e.*, near isothermal cooling) the sample to the crystallization temperature where gelation occurred. Quench cooling was completed using a linkham peltier plate. Each sample was crystallized at either 10, 15, 20, 25, or 30 °C. Enantiomeric D:L ratios of 12HSA, between 50 : 50 and 100 : 0, were prepared by mixing the enantiopure D-12HSA with the racemic DL-12HSA in appropriate proportions.

To obtain the synchrotron FTIR spectra, a drop of sol was placed between two hot CaF_2 optical windows (25 mm diameter, 2 mm thick) separated with a 15 μm Teflon spacer. The samples were then cooled on a Linkam LTS120 controlled temperature stage (Linkam, Surrey, United Kingdom) pre-set at 10, 15, 20, 25, or 30 °C. The samples were reused for each crystallization temperature. The typical heating protocol would include holding the sample at 100 °C for 30 min to ensure that the crystal history was erased. The sample was then quench cooled to the first crystallization temperature (*i.e.*, 10 °C) and held for 30–45 min depending on how long it took for the crystallization process to be completed. Following the 30–45 min hold the sample was re-heated to 90 °C and held once again for 30 min, ensuring the crystal history was erased. At this point, the temperature was quenched to the second crystallization temperature and held. This was carried out for all five crystallization temperatures and

then the samples were replaced for the second and third replicates.

Discussion

The enantiomeric nature of 12HSA, whether it is optically pure or racemic, has been found to have a significant effect on its critical concentration for gelation (cgc) of liquids. The critical concentration of the D-enantiomer in mineral oil was found to be between 0.5 and 1 wt % (Supporting Information File Figure S1), agreeing well with literature values.[7] However, the cgc of DL-12HSA was much higher, *ca.* 2.0 wt %, in mineral oil (Supporting Information File Figure S1). Recently, it was reported that ~2 wt % DL-12-HSA was unable to gelate benzene.[1b] Although this may be, in part, because the cgc in benzene is >2 wt %, the authors were able to gelate benzene easily with *ca.* ~1.3 wt % of the D- or L-enantiomer.

To explore further the dependence of the gelating ability of 12HSA on its enantiomeric content, 2.5 wt % samples were prepared in mineral oil with D:L enantiomeric ratios varying from 50 : 50 to 100 : 0 (Supporting Information File Figure S2). The appearance of the organogels depended acutely on the enantiomeric content. The pure D-12HSA gel was transparent while those containing 1 : 1 (racemic) up to *ca.* 80 : 20 D:L mixtures were visually opaque. Gels with D:L ratios >90 : 10 were less opaque, but not as transparent as the optically pure sample. The opacity of an organogel is directly related to the cross-sectional thickness of the crystalline aggregates, the number of junction zones capable of diffracting light, and the number of crystalline aggregates within the self-assembled network.[8]

Bright field micrographs (Fig. 1) and polarized light micrographs (ESI,† Fig. S3) provided information about the shapes of the crystalline objects constituting the SAFiNs within the gels. The transparent gels with *enantio*-pure D-12HSA produced long, twisted fibers (ESI,† Fig. S3K, L and Fig. 1 K, L). Although difficult to discern from the photomicrographs provided, fiber helicity was evident in the SAFiNs at D:L ratios at and above 90 : 10 (ESI,† Fig. S3I, J and Fig. 1I, J).[9] The SAFiNs of the opaque gels were comprised of platelet crystallites that are capable of diffracting light more than the helical fibers.[4h,10]

According to FT-IR spectra of the 12HSA gel phase, the volume of the solid phase scales proportionally to the hydroxyl stretching region (Fig. 2).[4f,7b] The molten sols at 90 °C for the various D:L mixtures were used as the background for subsequent spectra collected during crystallization. The samples were cooled rapidly from the sol phases to different crystallization temperatures below the sol–gel transition temperatures and spectra were recorded every 11 s in both the hydroxyl (Fig. 2) and carboxyl regions (Fig. 3). Differences in the spectral features are most evident between samples containing D:L ratios greater than and less than 80 : 20. For samples with D:L ratios in the range of 50 : 50 to 80 : 20, the hydroxyl hydrogen-bonding peak occurred at 3400 cm^{-1} (Fig. 2A–D). Samples with D:L ratios at or above 80 : 20 showed a doublet at 3300 and 3200 cm^{-1} (Fig. 2E–H). Similar results were reported using solid-state NMR where two types of hydrogen bonding were reported for D-HSA and DL-HSA, however ratios between 50 : 50 DL-HSA and 100 : 0 DL-HSA were not previously examined.[1b]

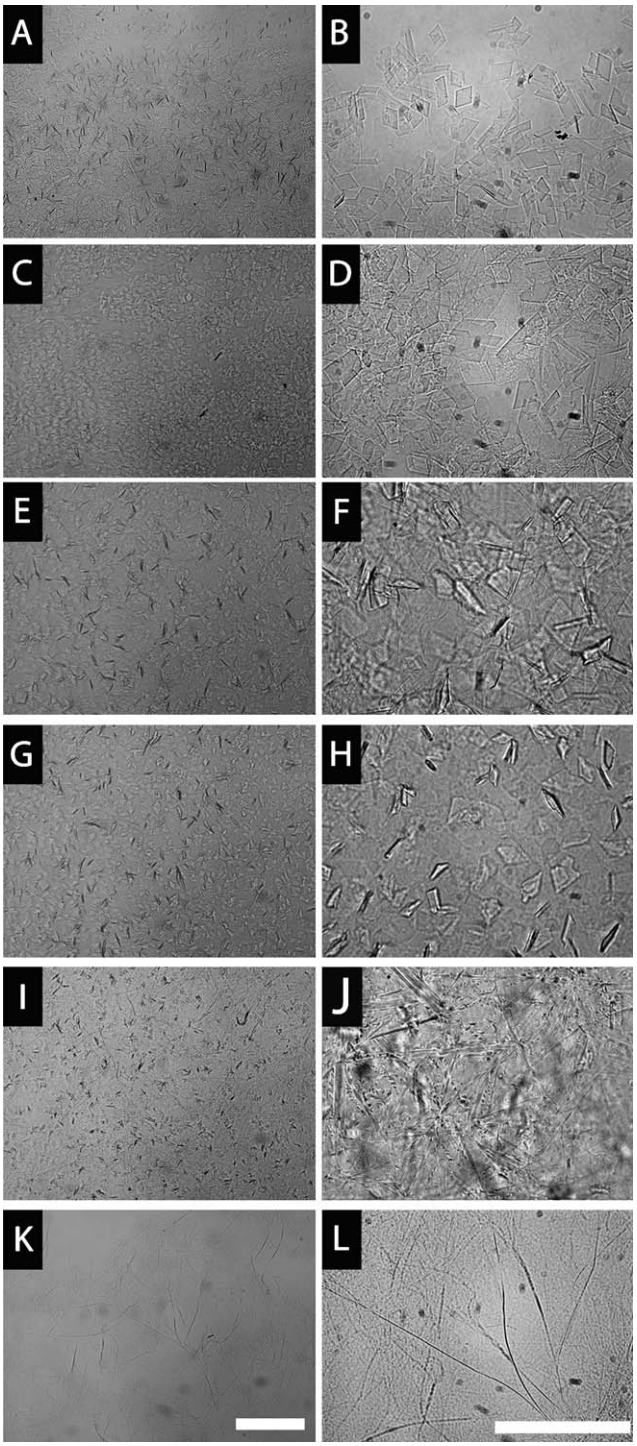

Fig. 1 Brightfield micrographs of (A,B) 50 : 50, (C,D) 60 : 40, (E,F) 70 : 30, (G,H) 80 : 20, (I,J) and 90 : 10 D:L-12HSA, and (K,L) D-12HSA. Magnification at 10X (A,C,E,G,I,K) and 40X (B,D,F,H,J,L). (Magnification bar = 20um).

The area associated with the hydroxyl hydrogen-bonding peaks (Fig. 2) was integrated between 3050 and 3550 cm^{-1} and plotted as a function of time at each of the incubation temperatures (Fig. 4). The sigmoidal curves, typical of crystallization events, were fitted to the Avrami equation (eqn (1))[11] as shown in Fig. 4 to determine the Avrami exponent (Fig. 5A) and the

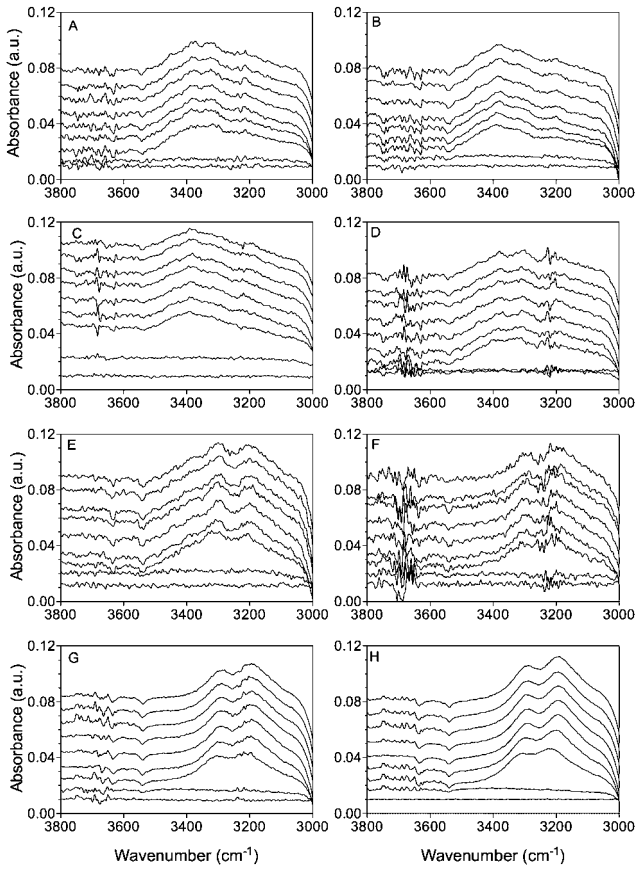

Fig. 2 Differential FT-IR spectra of the hydroxyl stretching regions of 12HSA assemblies during near-isothermal crystallization at 30 °C over a 20 min period for (A) 50 : 50, (B) 55 : 45, (C) 60 : 40, (D) 70 : 30, (E) 80 : 20, (F) 90 : 10, and (G) 95 : 05 DL-12HSA, and (H) 100 D-12HSA.

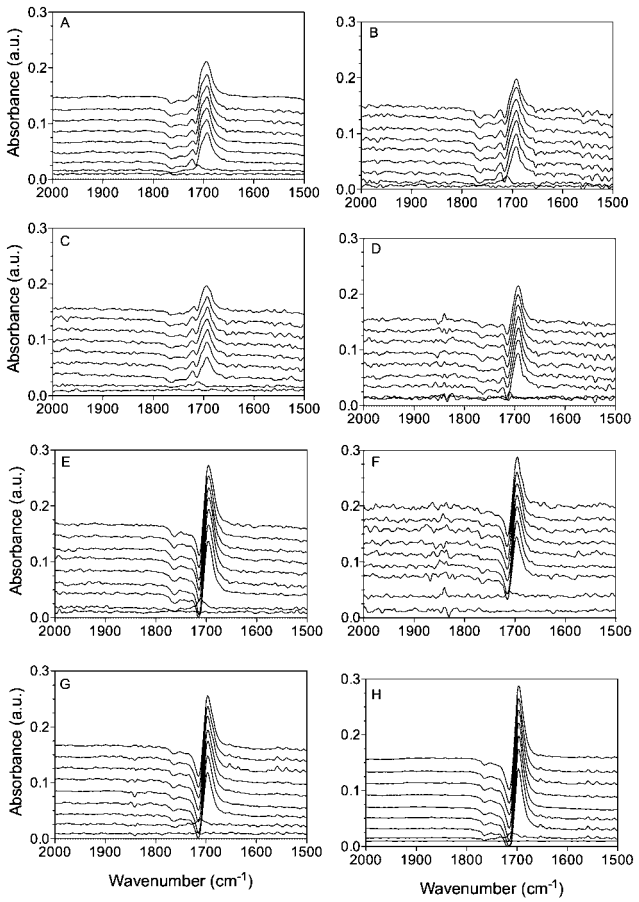

Fig. 3 Differential FT-IR spectra for the carboxylic acid region of 12HSA assembly during near-isothermal cooling to 30 °C over a 20 min period for (A) 50 : 50 DL-12HSA, (B) 55 : 45 DL-12HSA, (C) 60 : 40 DL-12HSA, (D) 70 : 30 DL-12HSA, (E) 80 : 20 DL-12HSA, (F) 90 : 10 DL-12HSA, (G) 95 : 05 DL-12HSA, (H) 100 D-12HSA.

Avrami rate constant (Fig. 5B). In eqn (1), Y is the phase volume (*i.e.*, the area under the 3200 cm^{-1} peak), k is the rate constant, x is time, and n is the Avrami exponent. The Avrami model has been utilized previously to analyze the kinetics and mode of gelation in other systems,[12] and has been used recently to model the crystallization process of D-12HSA organogels.[4b,4f]

$$Y = 1 - e^{-k(x)^n} \quad (1)$$

The Avrami exponent is a measure of the type of nucleation and dimensionality of crystal growth and typically has an integer value between 1 and 4. The values of n did not change over the range of crystallization temperatures explored with each of the 12HSA samples. For D:L ratios of 12HSA less than 80 : 20, n is equal to 3 (Fig. 5A), which corresponds either to platelet-like crystals and sporadic nucleation or spherulitic crystals and instantaneous nucleation.[11,13] The bright field micrographs (Fig. 1) and polarized light micrographs (ESI,† Fig. S3) along with the Avrami exponent are consistent with crystallization yielding platelet-like objects that have undergone sporadic nucleation. However, at D:L ratios above 80 : 20, an Avrami exponent of 2 is calculated (Fig. 5A), and the fiber morphology observed in Fig. 1 and S3 indicate that the crystallization process involves fiber-like crystal growth and sporadic nucleation.

The rate constants from the Avrami fits (k) can be plotted in an Arrhenius fashion (eqn (2)) to calculate activation energies of crystallization (Fig. 5C).

$$\ln k = \ln A + \frac{E_a}{RT} \quad (2)$$

where ln A is the y-intercept, E_a is the activation energy, R is the ideal gas constant and T is an incubation temperature corresponding to a value of k. The activation energy may only be calculated in this way if the dimensionality of growth, n, is the same at each incubation temperature (as it is here). A linear regression between the ln k *versus* the inverse of temperature yielded R^2 values greater than 0.88 for all fits (Fig. 5B). Interestingly, the calculated activation energy for nucleation was lower for fiber-formation than for platelet formation. The activation energy, a measure of the rate limiting step, may relate to the ease of phase separation in the sol state, ability of gelator molecules to accrete onto the early nuclei surface, or the ability of a gelator molecule to adapt the ideal molecular conformation to add to a crystal face; because, the chemical potentials of the enantiomeric mixtures of the 12HSA are must be nearly identical, the decision to form platelets or fibers must be made at the early stages of phase separation, nucleation, or growth. This is

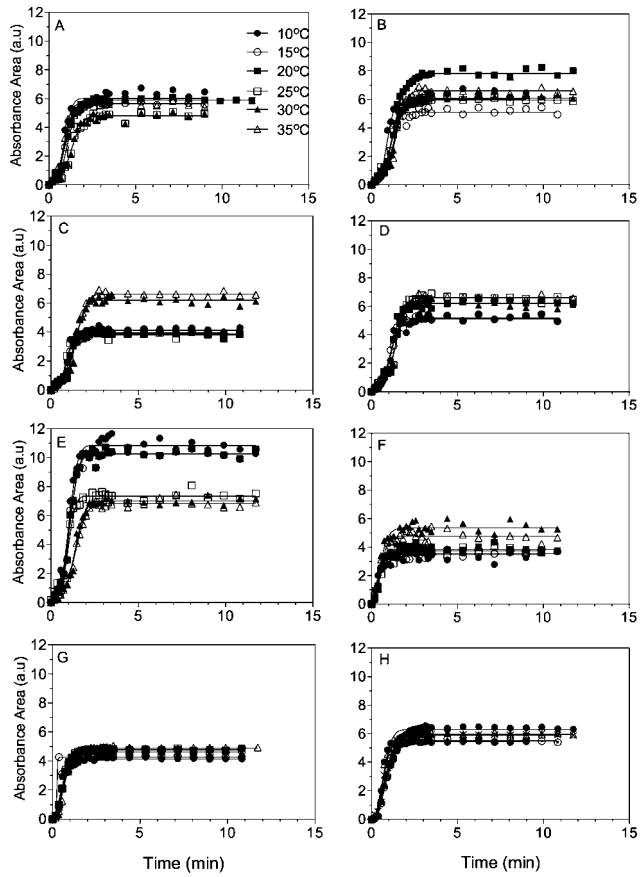

Fig. 4 Integrated areas of the FT-IR peaks in the 3000 to 3200 cm^{-1} spectral regions for (A) 50 : 50, (B) 55 : 45, (C) 60 : 40, (D) 70 : 30, (E) 80 : 20, (F) 90 : 10, and (G) 95 : 05 DL-12HSA, and (H) D-12HSA.

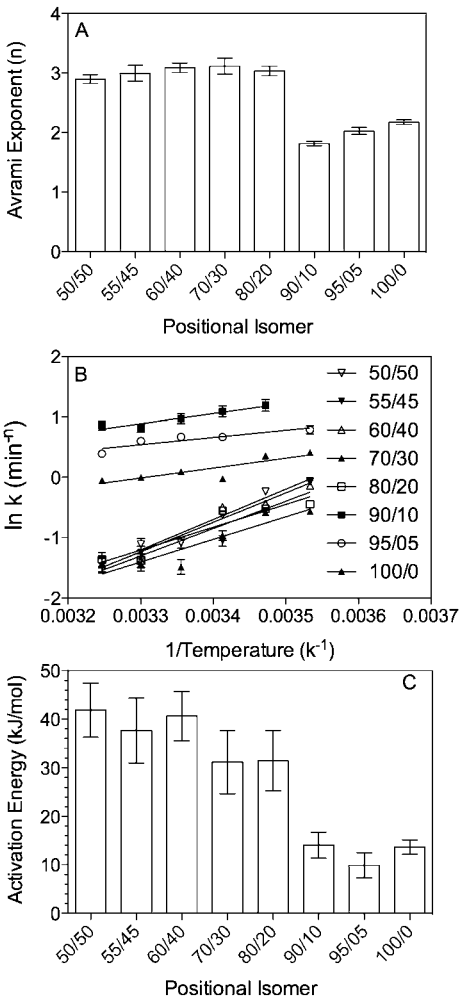

Fig. 5 Avrami exponents (A) and rate constants (B) using the Avrami equation and the 3200 cm^{-1} peak areas in FT-IR spectra. The activation energy (C) calculated using the rate constants from the Avrami model.

likely during the initial association of the hydroxylated fatty acids. The higher activation energy observed for platelet formation (*i.e.*, at DL ratios between 50 : 50 and 80 : 20) may be attributed to the fact that D-HSA pairs and D-HSA/L-HSA pairs of molecules must recognize each other *via* diastereomeric interactions. The latter may allow for the formation of more highly ordered aggregates,[1b] causing two dimensional platelets to be formed rather than one dimensional fibers found from the 12HSA at >80 : 20 ratios.

The FT-IR spectra in the region of carboxylic acid absorptions (Fig. 3) were analyzed carefully in order to gain insights into the molecular arrangements within the fibers and platelets. A small peak at approximately 1720 cm^{-1} is observable only at D:L ratios below 80 : 20 (Fig. 3 A–D), and there is a depletion of the signal intensity at 1730 cm^{-1} at ratios higher than 80 : 20 (Fig. 3E–H). Furthermore, all of the spectra, regardless of the D:L ratio, have a peak at 1700 cm^{-1}. The loss of signal intensity at 1730 cm^{-1} is associated with a decrease in the amount of (free) monomeric 12HSA, while the peak at 1700 cm^{-1} has been ascribed to the cyclic dimer of carboxylic acid head groups (Fig. 6).[14] The small peak at 1720 cm^{-1} corresponds to single in-plane hydrogen-bonded acyclic dimers (Fig. 6).[14] To confirm the presence of the different dimerization modes of the carboxylic head groups, the contribution from mineral oil was subtracted from the FT-IR spectra of the gels (Fig. 7). At D:L ratios lower than 80 : 20, there are equal amounts of cyclic and acyclic dimers; D-12HSA, and 95 : 05 and 90 : 10 DL-12HSA have significantly more cyclic than acyclic dimers (Fig. 7).

In gels with optically pure 12HSA, the hydroxyl groups are positioned on opposite sides of the cyclic dimer. Thus, hydroxyl hydrogen-bonding along the transverse axis promotes longitudinal growth. The racemic DL-12HSA mixture is more likely to form single, in-plane hydrogen-bonded acyclic dimers (Fig. 8)

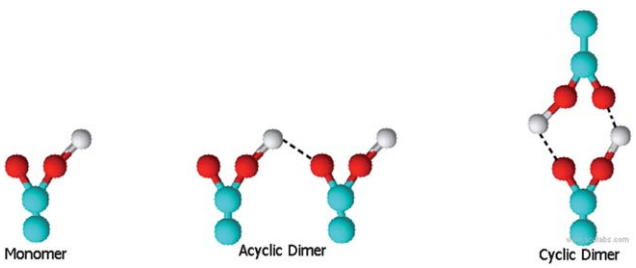

Fig. 6 Diagram of the free carboxylic acid monomer, acyclic carboxylic acid dimer and cyclic carboxylic acid dimer.

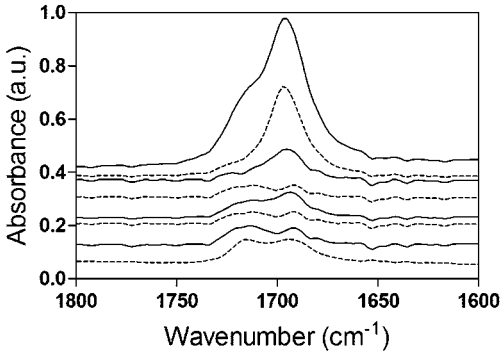

Fig. 7 FT-IR spectra associated with the carboxylic acid region of 12HSA for (from bottom to top) 50 : 50, 55 : 45, 60 : 40, 70 : 30, 80 : 20, 90 : 10, and 95 : 05 DL-12HSA and D-D-12HSA.

which allows additional H-bonding of the 12-hydroxyl groups within each dimer. However, the acyclic dimer does not facilitate longitudinal growth along the transverse axis; it favors growth of platelets.

During the early stages of nucleation and crystal growth, monomers of 12HSA dimerize causing microscopic phase separation of the polar carboxylic head group from the low polarity solvent in an attempt to reduce the interfacial tension. Upon sufficient under-cooling the Brownian forces become weaker and the non-covalent forces allow the formation of a stable crystal embryo. As crystallization progress free monomers and dimers diffuse to the embryo surface and accrete onto the surface. The formation of the cyclic dimer effectively shields the carboxylic acid groups from the low polarity regions within the SAFiNs. This, coupled with the necessity for a 12-hydroxyl group to form H-bonds with other immediately adjacent 12-hydroxyl groups, shields the polar groups of optically pure 12HSA from the low polarity solvent and, consequently, leads to a large reduction in the chemical potential and a lower activation energy (Fig. 5B). The acyclic dimer cannot effectively shield the polar head groups from the mineral oil, and results in a higher chemical potential and thus larger activation energy.

Conclusions

Although less than 1.0 wt % of (optically pure) D-12HSA was needed to form an organogel in mineral oil, 2.0 wt % of (racemic) DL-12HSA was required to effect gelation. The SAFiN of the optically pure gel was comprised of high aspect ratio fibers in which the D-12HSA molecules formed cyclic dimers between carboxyl groups and H-bonding of the 12-hydroxyl groups along the transverse axis favored longitudinal growth. The SAFiN of the DL-12HSA organogel was comprised of platelet-like interlocking crystals with a molecular arrangement of single in-plane hydrogen bonded acyclic dimers which prevent longitudinal growth and limit the ability of the polar groups to be shielded from the low polarity mineral oil solvent during nucleation. This difference may be the source of the higher the activation energy for nucleation and growth of the platelets than for fiber formation.

Acknowledgements

SA and RGW thank the US National Science Foundation for its support of the research performed at Georgetown. A portion of the research described in this paper was performed at the Canadian Light Source, which is supported by NSERC, NRC, CIHR, and the University of Saskatchewan. The authors are grateful to Tim May (CLS) for beamline design, construction and for constant help in beamline upkeep.

References

1 (*a*) P. Terech, V. Rodriguez, J. D. Barnes and G. B. McKenna, Organogels and Areogels of Racemic and Chiral 12-Hydroxyoctadecanoic Acid, *Langmuir*, 1994, **10**(10), 3406–3418; (*b*) T. Sakurai, Y. Masuda, H. Sato, A. Yamagishi, H. Kawaji, T. Atake and K. Hori, A Comparative Study on Chiral and Racemic 12-Hydroxyoctadecanoic Acids in the Slutions and Aggregation States: Does the Racemic Form Really Form a Gel?, *Bulletin of the Chemical Society of Japan*, 2010, **83**(2), 145–149.
2 R. G. Weiss, P. Terech, *Introduction. In Molecular Gels: Materials with Self-Assebled Fibrillar Networks*, Weiss R. G., Terech P., ed. Springer: Dordrecht, The Neatherlands, 2006; pp 1–13.
3 A. Brizard, R. Oda and I. Huc, Chirality Effects in Self-Assembled Fibrillar Networks, *Topic is Current Chemistry*, 2005, **256**, 167–215.

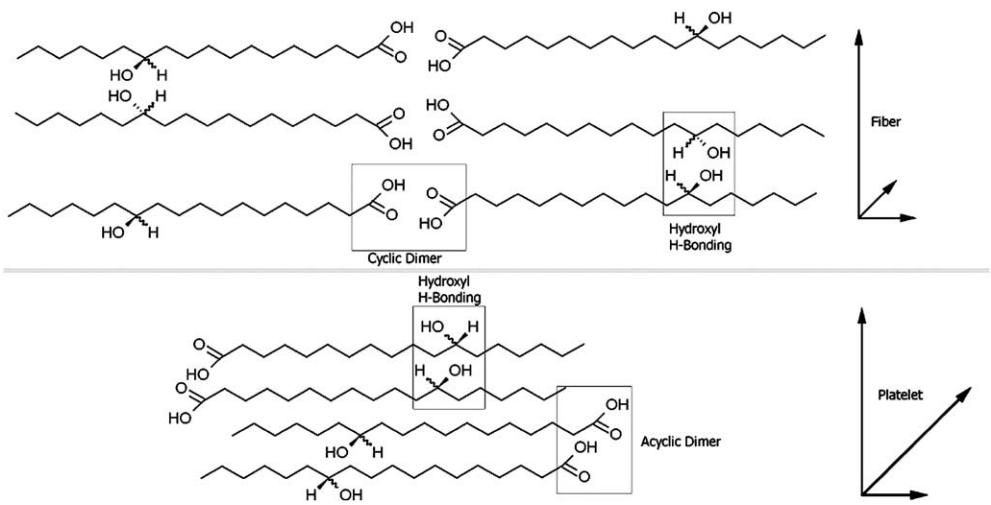

Fig. 8 Schematic representations of D-12HSA packing and DL-12HSA packing in SAFiNs of mineral oil gels.

4 (*a*) M. A. Rogers and A. G. Marangoni, Non-Isothermal Nucleation and Crystallization of 12-Hydroxystearic Acid in Vegetable Oils, *Crystal Growth & Design*, 2008, **8**(12), 4596–4601; (*b*) M. A. Rogers and A. G. Marangoni, Solvent-Modulated Nucleation and Crystallization Kinetics of 12-Hydroxystearic Acid: A Nonisothermal Approach, *Langmuir*, 2009, **25**(15), 8556–8566; (*c*) M. A. Rogers, T. Pedersen and L. Quaroni, Hydrogen-Bonding Density of Supramolecular Self-Assembled Fibrillar Networks Probed Using Synchrotron Infrared Spectromicroscopy, *Crystal Growth & Design*, 2009, **9**(8), 3621–3625; (*d*) V. A. Mallia, M. George, D. L. Blair and R. G. Weiss, Robust Organogels from Nitrogen-Containing Derivatives of (R)-12-Hydroxystearic Acid as Gelators: Comparisons with Gels from Stearic Acid Derivatives, *Langmuir*, 2009, **25**(15), 8615–8625; (*e*) J. L. Li, R. Y. Wang, X. Y. Liu and H. H. Pan, Nanoengineering of a Biocompatible Organogel by Thermal Processing, *Journal of Physical Chemistry B*, 2009, **113**(15), 5011–5015; (*f*) R. Lam, L. Quaroni, T. Pederson and M. A. Rogers, A molecular insight into the nature of crystallographic mismatches in self-assembled fibrillar networks under non-isothermal crystallization conditions, *Soft Matter*, 2010, **6**(2), 404–408; (*g*) T. Tachibana and H. Kambara, Sense of twist in fibrous aggregates from 12-hydroxystearic acid and its alkali metal soaps, *J. Colloid Interface Sci.*, 1968, **28**(1), 173–178; (*h*) T. Tachibana, T. Mori and K. Hori, Chiral Mesophases of 12-Hydroxyoctadecanoic Acid in Jelly and in the Solid State. I. A New Type of Lyotropic Mesophase in Jelly with Organic Solvents, *Bulletin of the Chemical Society of Japan*, 1980, **53**, 1714–1719; (*i*) T. Tachibana, A. Yamagishi and K. Hiro, Monolayer Studies of Chiral and Racemic 12-Hydroxyoctadecanoic Acids, *Bulletin of the Chemical Society of Japan*, 1979, **52**, 346–350; (*j*) P. Terech, 12-D-Hydroxyoctadecanoic Acid Organogels - A Small-Angle Neutron-Scattering Study, *J. Phys. II*, 1992, **2**(12), 2181–2195.

5 (*a*) X. Y. Liu and P. D. Sawant, Determination of the Fractal Characteristic of Nanofiber-Network Formation in Supramolecular Materials, *CHEMPHYSCHEM*, 2002, **4**, 374–377; (*b*) J. L. Li, X. Y. Liu, R. Y. Wang and J. Y. Xiong, Arichitecture of a Biocompatible Supramolecular Material by Supersaturation-Driven Fabrication of its Network, *Journal of Physical Chemistry B*, 2005, **109**, 24231–24235.

6 F. M. Menger, S. D. Richardson, M. G. Wood and M. J. Sherrod, Chain-Substituted Lipids in Monomolecular Films. Effect of Polar Substituents on Molecular Packing, *Langmuir*, 1989, **5**, 833–838.

7 (*a*) J. P. Eloundou, E. Girard-Reydet, J. F. Gerard and J. P. Pascualt, Calorimetric and Rheological Studies of 12-Hydroxystearic Acid/Digycidyl Ether of Biophenol A Blends, *Polymer Bulletin*, 2005, **53**, 367–375; (*b*) M. A. Rogers, A. J. Wright and A. G. Marangoni, Engineering the oil binding capacity and crystallinity of self-assembled fibrillar networks of 12-hydroxystearic acid in edible oils, *Soft Matter*, 2008, **4**(7), 1483–1490; (*c*) M. A. Rogers, A. J. Wright and A. G. Marangoni, Nanostructuring fiber morphology and solvent inclusions in 12-hydroxystearic acid/canola oil organogels (vol. 14, pg 33, 2009), *Current Opinion in Colloid & Interface Science*, 2009, **14**(3), 223–223.

8 (*a*) P. Terech, D. Pasquier, V. Bordas and C. Rossat, Rheological properties and structural correlations in molecular gels, *Langmuir*, 2000, **16**, 4485–4494; (*b*) T. Tamura and M. Ichikawa, Effect of lecithin on organogel formation of 12-hydroxystearic acid, *Journal of the American Oil Chemists Society*, 1997, **74**(5), 491–495.

9 (*a*) R. Oda, I. Huc, M. Schmutz, S. J. Candau and F. C. MacKintosh, Tuning Bilayer Twist Using Chiral Couterions, *Nature*, 1999, **399**, 566–569; (*b*) A. Brizard, D. Berthier, C. Aime, T. Buffeteau, D. Cavagnat, L. Ducasse, I. Huc and R. Oda, Molcular and Supramolecular Chirality in Gemini-Tartrate Amphiphiles Studies by Electronic and Vibrational Circular Dichroisms, *Chirality*, 2009, **21**, E153–E152.

10 (*a*) J. H. Fuhrhop, P. Schnieder, J. Rosenberg and E. Boekema, The Chiral Bilayer Effect Stabilized Micellar Fibers, *Journal of the American Chemical Society*, 1987, **109**, 3387–3390; (*b*) T. Tachibana, T. Mori and K. Hori, Chiral Mesophases of 12-Hydroxyoctadecanoic Acid in Jelly and in the Solid State. II. A New Type of Mesomorphic Solid State, *Bulletin of the Chemical Society of Japan*, 1981, **54**, 7.

11 (*a*) M. Avrami, Kinetics of Phase Change. I. General Theory, *Journal of Chemical Physics*, 1939, **7**(12), 1103–1112; (*b*) M. Avrami, Kinetics of Phase Change. II. Transformation-Time Relations for Random Distribution of Nuclei, *Journal of Chemical Physics*, 1940, **8**(22), 212–226; (*c*) M. Avrami, Kinetics of Phase Change. III. Granulation, Phase Change, and Microstructure, *Journal of Chemical Physics*, 1941, **9**(2), 177–184.

12 (*a*) X. Huang, S. R. Raghavan, P. Terech and R. G. Weiss, Distinct Kinetic Pathways Generate Organogel Networks with Contrasting Fractality and Thixotopic Properties, *Journal of the American Chemical Society*, 2006, **128**, 15341–15352; (*b*) P. Terech, Kinetics of Aggregation in a Steroid Derivative/Cyclohexane Gelifying System, *J. Colloid Interface Sci.*, 1985, **107**(1), 244–255.

13 R. S. H. Lam and M. A. Rogers, Experimental Validation of the Modified Avrami Model for Non-Isothermal Crystallization Conditions, *Crystal Engineering Communications*, 2010, **13**, 866–875.

14 (*a*) R. Arnold, W. Azzam, A. Terfort and C. Woll, Preparation, Modification, and Crystallinity of Aliphatic and Aromatic Carboxylic Acid Therminated Self-Assembled Monolayers, *Langmuir*, 2002, **18**, 3980–3983; (*b*) R. G. Nuzzo, L. H. Dubois and D. L. Allara, Fundamental Studies of Microscopic Wetting on Organic Surfaces. 1. Formation and Structural Characterization of a Self-Consistent Series of Polyfuntional Organic Monolayers, *Journal of the American Chemical Society*, 1990, **112**, 558–563.